HEDN: A Hard-Easy Dual Network with Task Difficulty Assessment for EEG Emotion Recognition

Qiang Wang, Liying Yang

School of Computer Science and Technology, Xidian University, Xi'an, China Email: qiang.wang@stu.xidian.edu.cn, yangliying1208@163.com

Abstract—Multi-source domain adaptation represents an effective approach to addressing individual differences in cross-subject EEG emotion recognition. However, existing methods treat all source domains equally, neglecting the varying transfer difficulties between different source domains and the target domain. This oversight can lead to suboptimal adaptation. To address this challenge, we propose a novel Hard-Easy Dual Network (HEDN), which dynamically identifies "Hard Source" and "Easy Source" through a Task Difficulty Assessment (TDA) mechanism and establishes two specialized knowledge adaptation branches. Specifically, the Hard Network is dedicated to handling "Hard Source" with higher transfer difficulty by aligning marginal distribution differences between source and target domains. Conversely, the Easy Network focuses on "Easy Source" with low transfer difficulty, utilizing a prototype classifier to model intra-class clustering structures while generating reliable pseudolabels for the target domain through a prototype-guided label propagation algorithm. Extensive experiments on two benchmark datasets, SEED and SEED-IV, demonstrate that HEDN achieves state-of-the-art performance in cross-subject EEG emotion recognition, with average accuracies of 93.58% on SEED and 79.82% on SEED-IV, respectively. These results confirm the effectiveness and generalizability of HEDN in cross-subject EEG emotion recognition.

Index Terms-EEG; Emotion Recognition; Transfer Learning.

I. INTRODUCTION

Understanding human emotional states plays a crucial role in the development of intelligent systems for affective computing, especially in applications such as personalized human-computer interaction [1] and mental health monitoring [2]. Among various physiological signals, electroencephalography (EEG) provides a direct, non-invasive, and temporally precise window into the brain's emotional and cognitive processes [3]. These characteristics make EEG emotion recognition a promising and challenging task in artificial intelligence.

However, individual differences in neuroanatomy and emotional expression result in significant distributional discrepancies in EEG signals collected from different subjects [4]–[6]. This inter-subject variability limits model generalization and hinders deployment in real-world applications. Domain adaptation (DA) has emerged as a prominent research direction in cross-subject EEG emotion recognition, aligning source domains (subjects with labeled data) and target domains

Negative
Neutral
Positive

(a) SEED Subject 1

(b) SEED Subject 2

Happy
Sad
Neutral
Fear
(c) SEED-IV Subject 1

(d) SEED-IV Subject 2

Fig. 1. t-SNE visualizations showing intra-subject heterogeneity in EEG emotion recognition. Multi-cluster structures within each emotional state are observed across (a-b) SEED dataset subjects and (c-d) SEED-IV dataset subjects, demonstrating complex intra-class variability.

(subjects without labels) distributions to improve generalization [7]. Multi-source domain adaptation (MSDA), a natural extension of single-source DA [8], independently models each source-target pair. This addresses a key limitation of single-source methods that problematically assume a unified source distribution, which is particularly problematic in cross-subject EEG [9], [10]. However, existing MSDA methods often suffer from two critical limitations: First, they treat all source domains equally, ignoring varying transfer difficulties between source-target pairs [11]. This uniform treatment can lead to negative transfer when some sources are poorly aligned [12]. Second, independent adaptation branches for each source increase computational and storage overhead, incompatible with low-latency Brain-Computer Interface (BCI) requirements.

Beyond inter-subject variability, another critical challenge lies in the intra-subject heterogeneity in emotional expression [13], as illustrated in Figure 1. The t-SNE visualizations [14] reveal that even within identical emotional states, EEG signals from individual subjects exhibit distinct multi-cluster structures across different datasets. For instance, in the SEED dataset with three emotional categories (negative, neutral, pos-

itive), each emotional state shows complex clustering patterns that vary between subjects. These intra-class structures carry rich semantic information, yet most existing domain adaptation methods ignore such latent structures, missing the opportunity to align data at a finer granularity.

To address the above challenges, we propose a novel Hard-Easy Dual Network (HEDN) framework, inspired by curriculum learning [15] and theoretical insights on domain transferability [16]. We argue that varying levels of transfer difficulty require fundamentally different adaptation strategies, as source domains differ in their compatibility with the target domain. Specifically, the "Hard Source" with high transfer difficulty benefit from marginal distribution alignment through adversarial training, while the "Easy Source" with better compatibility can leverage structural modeling and prototype-based classification for more stable knowledge transfer. Thus, HEDN incorporates a Task Difficulty Assessment (TDA) mechanism to dynamically evaluate source domain transferability during training. Based on the assessed difficulty, HEDN routes different sources to specialized processing pathways. The Hard Network mitigates negative transfer from challenging sources by aligning marginal distributions via adversarial learning, while the Easy Network leverages intra-class structural information from compatible sources using prototype-based representation and label propagation. Furthermore, to address the intrasubject heterogeneity, we incorporate a prototype-guided label propagation strategy that exploits latent clustering structures to generate reliable pseudo-labels, enabling principled and effective adaptation. Finally, to fully leverage HEDN's advantages without interference among loss components, we design a stepwise joint optimization strategy.

The main contributions of this paper are summarized as follows:

- We propose a HEDN framework for cross-subject EEG emotion recognition, which dynamically routes source domains with different transfer difficulties to specialized adaptation pathways, enabling more effective and targeted knowledge transfer.
- We introduce a TDA mechanism that quantifies sourcetarget transferability by jointly considering classification loss and domain discrepancy, allowing the model to adaptively select hard and easy sources during training.
- We design a structure-aware adaptation strategy that incorporates prototype-guided label propagation and cluster contrastive learning, effectively leveraging intra-class semantic structures to enhance pseudo-label reliability.

II. RELATED WORK

A. Multi-Source Domain Adaptation

Multi-source domain adaptation extends traditional single-source settings by leveraging multiple labeled source domains to improve generalization on an unlabeled target domain. Early MSDA methods typically adopted a "source domain equality" strategy, treating all sources equally and aligning them with the target domain in a shared feature space [10], [17], [18]. For instance, MS-MDA [10] proposed shared-private feature extraction to separate domain-invariant and domain-specific

features, while S²A²-MSDA [18] first aligned global distributional shifts using spectral-spatial attention across all source and target domains, and then introduced dedicated modules to model each source-target pair individually. However, due to the substantial distributional discrepancies between different source and target domains, indiscriminately treating all source domains equally during training is likely to cause negative transfer [19], [20]. Some methods have attempted to address this through source selection strategies. MSGDAN [20] calculates Maximum Mean Discrepancy(MMD) distances to select highly similar source domains while eliminating those with high transfer difficulty. LSA-MMFT [19] employed Label Similarity Analysis(LSA) to evaluate transferability by assessing prediction consistency between source and target domains. Nevertheless, these selection-based approaches sacrifice potentially valuable source domain information and lack mechanisms to progressively address varying transfer difficulties.

In contrast, our method retains all source domains and introduces the TDA module that quantifies transferability based on classification and domain discrepancy. This dynamically selects both hard and easy source domains for joint adaptation, achieving more targeted and efficient transfer.

B. Prototype Learning

Prototype learning [21] aims to effectively capture global data structure by constructing center vectors (i.e., prototypes) in feature space that represent different data distributions, demonstrating strong robustness in handling label noise and intra-class variations. PR-PL [22] proposed a prototype representation and pairwise learning framework that represents emotion category centers through prototype features, thereby reducing individual differences and label noise effects. MSPR-GNN [23] developed a multi-source domain prototype graph network that establishes independent prototypes for each source domain, substantially improving cross-domain distribution alignment. ADANN [24] introduced dual prototype contrastive learning and adaptive conditional distribution alignment, significantly enhancing cross-subject EEG emotion recognition generalization. However, these methods primarily focus on constructing global prototypes for emotion categories while neglecting intra-class distributional structural differences, making it difficult to fully characterize potential diversity and clustering structures within source domains.

In contrast to existing approaches, our approach incorporates structure-aware prototype learning guided by clustering patterns within emotion categories. This enables finer-grained alignment and more reliable pseudo-label propagation, leading to improved robustness in cross-subject adaptation.

III. METHODS

In multi-source cross-subject EEG emotion recognition, we are given M labeled source domains $\mathcal{S} = \{\mathcal{D}_s^i\}_{i=1}^M$, where each source domain $\mathcal{D}_s^i = \{(x_j^i, y_j^i)\}_{j=1}^{N_t}$ contains N_i EEG samples from the i-th subject with corresponding emotion labels. The target domain $\mathcal{D}_t = \{x_j^t\}_{j=1}^{N_t}$ consists of N_t unlabeled EEG samples from a new subject. Our goal is to leverage knowledge

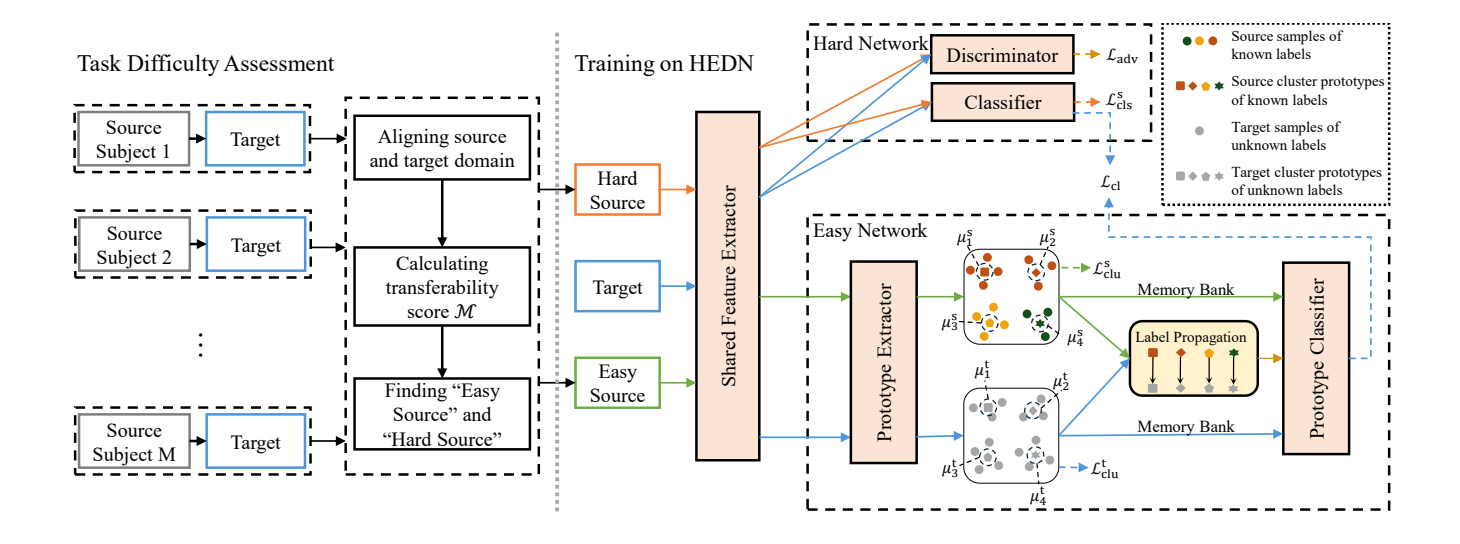


Fig. 2. Overall of the proposed HEDN framework. Multi-source domains undergo task difficulty assessment for dynamic routing to appropriate sub-networks, where Hard Network handles challenging transfers via adversarial training while Easy Network leverages clustering-based prototype learning for stable knowledge transfer. Both sharing a common feature extractor.

from multiple sources to train a robust classifier generalizing well to the target.

Figure 2 illustrates the overall architecture of the proposed framework HEDN. The framework comprises three main components: (1) a TDA module that dynamically evaluates the transferability; (2) a Hard Network for adversarial alignment of challenging sources; and (3) an Easy Network for structure-aware adaptation of compatible sources via prototype-guided learning. A shared feature extractor $f(\cdot)$ generates common representations for both networks. By dynamically routing source domains to the appropriate sub-network based on their estimated difficulty, HEDN enables targeted adaptation strategies that enhance overall transfer effectiveness.

A. Task Difficulty Assessment

To avoid uniform treatment of sources, we treat each source-target adaptation as an independent task, inspired by curriculum learning [15]. Adaptation tasks are dynamically sampled and progressively optimized.

Prior theoretical studies [16], [25] demonstrate that a source domain's generalization ability to the target can be jointly determined by the classification error and the distributional discrepancy. Specifically, for a hypothesis h on target distribution P with respect to the true labeling function f_P , its expected loss $\mathcal{L}_P(h, f_P)$ (target domain error) is bounded by:

$$\mathcal{L}_P(h, f_P) \le \mathcal{L}_Q(h, h_O^*) + \operatorname{disc}(P, Q) + \lambda(H, m, \delta), \quad (1)$$

where $\mathcal{L}_Q(h,h_Q^*)$ denotes the loss of hypothesis h on source distribution Q relative to its optimal hypothesis h_Q^* (i.e., source domain error); $\operatorname{disc}(P,Q)$ measures the distribution discrepancy between P and Q; and $\lambda(H,m,\delta)$ is an error term determined by the capacity of the hypothesis space H, the sample size m, and a confidence parameter δ . This bound guidance for assessment of source domain transferability: domains

with both low classification error and small distributional gaps are more likely to transfer successfully.

Guided by these insights, we propose a dynamic task difficulty assessment mechanism integrating classification loss and domain discrepancy. Specifically, we compute the classification loss \mathcal{L}_{cls} and adversarial loss \mathcal{L}_{adv} for each source domain using the Hard Network to quantify task error and domain misalignment, respectively. Since these losses exhibit significant differences in numerical scales and convergence characteristics, we employ a normalized weighted combination with a dynamic coefficient α to gradually shift from early-stage domain alignment to a focus on classification accuracy. For each source domain \mathcal{D}_s^i , we compute its transferability score \mathcal{M}_i as:

$$\mathcal{M}_i = \alpha \mathcal{L}_{cls}^i + (1 - \alpha) \mathcal{L}_{adv}^i, \tag{2}$$

where α is a dynamic weighting coefficient that evolves throughout training:

$$\alpha = \frac{1}{1 + \exp\left(-\frac{t - t_0}{\tau_1}\right)},\tag{3}$$

where t represents the current training epoch, t_0 the transition point, and τ_1 controlling transition smoothness.

At each iteration, the "Hard Source" $\mathcal{D}_{hard} = \arg\max_i \mathcal{M}_i$ and the "Easy Source" $\mathcal{D}_{easy} = \arg\min_i \mathcal{M}_i$ are selected for specialized adaptation.

B. Hard Network

The Hard Network is designed to address source domains with high transfer difficulty by aligning their marginal distributions with that of the target domain. We introduce Domain-Adversarial Neural Networks (DANN) [26] as the main module of the Hard Network, which consists of three subcomponents: an emotion classifier $h(\cdot)$, a domain discriminator

 $d(\cdot)$, and a shared feature extractor $f(\cdot)$ that is externally defined and reused across the framework. Here, $f(\cdot)$ extracts latent features from raw EEG signals, $h(\cdot)$ promotes emotion-discriminative representations, and $d(\cdot)$ learns to differentiate between source and target domain features through adversarial training, thereby guiding $f(\cdot)$ to produce domain-invariant representations. Additionally, to achieve end-to-end training, we employ a Gradient Reversal Layer (GRL) to coordinate the optimization process between feature extraction and adversarial training. The overall optimization objective is defined as:

$$\mathcal{L}_{\text{hard}} = \mathcal{L}_{\text{cls}}^s + \lambda_1 \mathcal{L}_{\text{adv}}, \tag{4}$$

where λ_1 is a hyperparameter that balances the contribution of the classification and adversarial losses, following the exponential growth schedule used in existing studies [22], [27]. $\mathcal{L}_{\text{cls}}^s$ represents the emotion classification loss for source domains, defined using cross-entropy as:

$$\mathcal{L}_{\text{cls}}^{s} = -\frac{1}{N_{s}} \sum_{i=1}^{N_{s}} y_{i} \log \left(h(f(x_{i}^{s})) \right), \tag{5}$$

and \mathcal{L}_{adv} represents the adversarial loss is defined as:

$$\mathcal{L}_{adv} = -\frac{1}{N_s} \sum_{i=1}^{N_s} \log d(f(x_i^s)) - \frac{1}{N_t} \sum_{i=1}^{N_t} \log(1 - d(f(x_i^t))),$$
(6)

where N_s and N_t are the number of samples in the source and target domains, respectively.

C. Easy Network

For sources with low transfer difficulty, the Easy Network exploits intra-class clustering to transfer class-conditional distributions. It combines a prototype feature extractor $g(\cdot)$ and prototype classifier $p(\cdot)$ with the shared feature extractor $f(\cdot)$. Two mechanisms drive fine-grained adaptation: prototype-guided label propagation and cluster-level contrastive learning.

1) Prototype-Guided Label Propagation: Inspired by DBPM [13], we design a prototype-guided label propagation strategy to generate high-quality target pseudo-labels. We begin by performing clustering analysis on both source and target domain samples independently to obtain cluster sets \mathcal{C}_s and \mathcal{C}_t for source and target domains, respectively. For this, we employ DBSCAN clustering (with specific parameters like ϵ and min_samples to be detailed in the Implementation Details section). DBSCAN is chosen for its ability to capture underlying EEG signal structure without requiring a predefined number of clusters [13], [28]. Samples within the same cluster typically correspond to consistent emotion categories. Thus, we construct a structured mapping from samples to categories through cluster label refinement: $\psi_s: \mathcal{X}_s \to \mathcal{C}_s \to \mathcal{Y}_s$, to refine source domain labels based on clustering.

To transfer category-level knowledge, the prototype classifier maintains prototype representations for each source and target cluster. Given prototypes μ_i^t and μ_j^s from target and source clusters respectively, we compute cosine similarity as:

$$sim(\mu_i^t, \mu_j^s) = \frac{\mu_i^t \cdot \mu_j^s}{\|\mu_i^t\|_2 \|\mu_j^s\|_2}.$$
 (7)

For each target cluster prototype μ_i^t , we identify the most similar source cluster prototype and assign its corresponding emotion category as the pseudo-label for the target cluster. This label is then propagated to all samples within the cluster. Accordingly, a pseudo-label mapping for the target domain is established as $\psi_t: \mathcal{X}_t \to \mathcal{C}_t \to \mathcal{Y}_s$, where each target sample is first associated with a target cluster and subsequently inherits the category label from its most similar source cluster. This process facilitates consistent and structure-aware pseudo-label propagation across domains.

To ensure that the prototypes are discriminative and temporally stable during training, we compute cluster prototypes based on semantic features extracted by g(f(x)). For any given set of samples, a prototype for the i-th cluster, $\hat{\mu}_i$, is calculated as the mean of its constituent sample features:

$$\hat{\mu}_i = \frac{1}{|\mathcal{C}_i|} \sum_{x_j \in \mathcal{C}_i} g(f(x_j)). \tag{8}$$

At the beginning of training, we initialize historical prototypes μ_i stored in the Memory Bank by setting them equal to the corresponding prototypes $\hat{\mu}_i$ computed from all available samples for each cluster. And in later training iterations, these historical prototypes are updated using an exponential moving average (EMA) strategy:

$$\mu_i = \gamma \mu_i + (1 - \gamma)\hat{\mu}_i,\tag{9}$$

where $\gamma \in [0,1)$ is a smoothing coefficient that balances the retention of previous prototype information μ_i with the incorporation of the current batch's prototype $\hat{\mu}_i$. Related studies [29], [30] have shown that this design improves model effectiveness by promoting stable and robust prototype representations.

2) Cluster Contrastive Learning: To further enhance the discriminability of clustering-based representations, we apply a cluster-level supervised contrastive loss [31]. This loss enforces intra-cluster compactness and inter-cluster separability, improving cluster quality and prototype reliability, which benefits pseudo-label propagation and cross-domain alignment.

Given a mini-batch of B samples, we obtain semantic features $\mathbf{z}_i = g(f(x_i))$ for each input x_i . Each \mathbf{z}_i is treated as an anchor, and its positive set $\mathcal{P}(i)$ includes all other samples in the batch with the same cluster label. The cluster contrastive loss is defined as:

$$\mathcal{L}_{\text{clu}} = -\frac{1}{B} \sum_{i=1}^{B} \frac{1}{|\mathcal{P}(i)|} \sum_{j \in \mathcal{P}(i)} \log \frac{\exp(s_{ij}/\tau_2)}{\sum_{k \neq i} \exp(s_{ik}/\tau_2)}, \quad (10)$$

where $s_{ij} = \cos(\mathbf{z}_i, \mathbf{z}_j)$ denotes cosine similarity and τ_2 is a temperature coefficient controlling sensitivity.

Algorithm 1 Training Algorithm of HEDN

Require: Source domains $S = \{\mathcal{D}^i\}_{i=1}^M$, target domain \mathcal{T} Ensure: Trained HEDN model

- 1: Perform DBSCAN on each \mathcal{D}^i and \mathcal{T} to obtain clusters C_s^i , C_t .
- 2: Compute and store initial cluster prototypes μ_c^s , μ_c^t in memory bank by Eq. (8).
- 3: for each training iteration do
- for each $\mathcal{D}^i \in \mathcal{S}$ do 4:
- Calculate task difficulty \mathcal{M}_i by Eq. (2). 5:
- 6:
- 7:
- Select $\mathcal{D}_{hard} = \arg \max_{i} \mathcal{M}_{i}$, $\mathcal{D}_{easy} = \arg \min_{i} \mathcal{M}_{i}$. Extract features $z^{e} = g(f(x^{e}))$, $z^{t} = g(f(x^{t}))$, update cluster prototypes μ^s and μ^t by Eq. (8) and (9).
- Compute main objective loss \mathcal{L}_{main} by Eq. (12). 9.
- Update parameters of $f(\cdot)$, $h(\cdot)$, and $d(\cdot)$. 10:
- Compute clustering contrastive loss $\mathcal{L}_{\text{struct}}$ by Eq. (10). 11:
- Update parameters of $g(\cdot)$. 12:
- 13: end for
- 14: return Trained HEDN model

D. Consistency Loss

To reduce prediction discrepancies between the Hard and Easy Networks on target samples, we introduce a Consistency Loss that aligns their outputs under pseudo-label supervision. Let $\hat{y}_{t,i}^h$ be the predicted probability from the Hard Network and $\hat{y}_{t,i}^e$ the pseudo-label from the Easy Network. The loss is defined as:

$$\mathcal{L}_{cl} = -\frac{1}{B} \sum_{i=1}^{B} \hat{y}_{t,i}^{e} \cdot \log \hat{y}_{t,i}^{h}, \tag{11}$$

where B is the batch size. This encourages prediction consistency between the two networks during joint training.

E. Step-wise Joint Optimization

To fully leverage the HEDN architecture while avoiding conflicts between different loss terms, we adapt a step-wise joint optimization strategy that alternates between transfer modeling and structural enhancement.

1) Step 1: Main Optimization: We first focus on transfer modeling by optimizing the classification loss $\mathcal{L}_{\text{cls}}^{s}$ and adversarial loss \mathcal{L}_{adv} for the Hard Network using the "Hard Source". Simultaneously, a consistency loss \mathcal{L}_{cl} aligns predictions between the Hard and Easy Networks on target samples. The overall loss is:

$$\mathcal{L}_{\text{main}} = \mathcal{L}_{\text{cls}}^s + \lambda_1 \mathcal{L}_{\text{adv}} + \lambda_2 \mathcal{L}_{\text{cl}}, \tag{12}$$

where λ_1 and λ_2 are balancing coefficients. This step mitigates marginal distribution shifts while promoting semantic consistency across networks.

2) Step 2: Structural Enhancement: Next, we apply cluster contrastive learning on the Easy Network's prototype extractor using the "Easy Source" and the target domain. The structural loss is:

$$\mathcal{L}_{\text{struct}} = \mathcal{L}_{\text{clu}}^{\text{s}} + \mathcal{L}_{\text{clu}}^{\text{t}}, \tag{13}$$

Algorithm 2 Prediction for Target Sample

Require: Target sample x^t ; target prototypes $\mathcal{U}_t = \{\mu_k^t\}$; source prototypes $\{\mathcal{U}_s^i\}_{i=1}^M$ with labels; trained $f(\cdot)$ and

Ensure: Predicted label \hat{y}^t

- 1: Extract semantic feature: $z^t = g(f(x^t))$.
- 2: Assign target cluster: $k^* = \arg\max_k \cos(z^t, \mu_k^t)$.
- 3: **for** i = 1 to M **do**
- For the assigned target cluster prototype $\mu_{k^*}^t$, find the most similar source prototype from domain \mathcal{D}^i :

$$j^* = \arg\max_{j} \cos(\mu_{k^*}^t, \mu_j^{s_i}).$$

- Collect corresponding label: $y_i = y_{i*}^{s_i}$.
- 6: end for
- 7: Final prediction by majority vote:

$$\hat{y}^t = \text{Vote}(\{y_i\}_{i=1}^M).$$

8: **return** \hat{y}^t

which improves cluster compactness and separability. During this step, only the Easy Network's prototype extractor $q(\cdot)$ is updated, preserving stability for the rest of the model. The specific algorithmic procedure is presented in Algorithm 1.

F. Prediction

Building upon the cluster-based prediction approach introduced by [32], we extend their methodology to enable effective cross-subject prediction through a structure-aware label transfer strategy. During the prediction stage, we employ the learned cluster prototypes to transfer knowledge across domains. Given a target sample, we first extract its semantic feature and assign it to the nearest target cluster prototype. For this cluster, we identify the most similar prototype from each source domain and collect their associated labels. The final prediction for the sample is obtained via majority voting among these labels. The specific algorithmic procedure is presented in Algorithm 2.

IV. EXPERIMENT

A. Datasets

We evaluate the performance of HEDN on two public EEG emotion datasets: SEED [33] and SEED-IV [34], which record EEG responses to movie clips eliciting emotions. The SEED includes 15 clips across three categories (positive, negative, neutral). The SEED-IV contains 24 clips spanning four categories (happy, sad, neutral, fearful). The experiments were conducted across three separate sessions.

EEG data were collected via the ESI NeuroScan system using 62 electrodes (10-20 system). Signals were bandpass filtered (0–75 Hz), and differential entropy (DE) features were extracted over five frequency bands: δ (1–3 Hz), θ (4–7 Hz), α (8–13 Hz), β (14–30 Hz), and γ (31–50 Hz), yielding 310-dimensional (62 channels \times 5 frequency bands) features per sample [35]. Regarding sample quantities, each session in the SEED dataset contains 3,394 samples, while the SEED-IV dataset contains 851, 832, and 822 samples in the three sessions, respectively.

B. Implementation Details

Regarding hyperparameters, we adapt the RMSprop optimizer with a learning rate of 1e-3 and a weight decay coefficient of 1e-5. The maximum number of training iterations is set to 1000. Due to the different data scales of SEED and SEED-IV, batch sizes are set to 96 and 64, respectively. We set t_0 and τ_1 to 100 for the dynamic weighting strategy. In the main objective loss, balancing coefficient λ_2 is set to 0.01. The prototype update momentum γ is set to 0.5, and the clustering temperature τ_2 is set to 1. For DBSCAN clustering, ϵ is set to 1 and min_samples is set to 5. To ensure reproducibility, the random seed is fixed at 42. All experiments are implemented using PyTorch and conducted on an NVIDIA RTX 5070Ti GPU.

C. Experimental Results

TABLE I
PERFORMANCE OF OUR PROPOSED HEDN COMPARED TO
STATE-OF-THE-ART APPROACHES.

Methods	SEED(%)	SEED-IV(%)
UDDA	88.10±06.54	73.14±09.43
MS-MDA	89.63 ± 06.79	59.34 ± 05.48
MSDA-SFE	91.65 ± 02.91	73.92 ± 06.04
S^2A^2 -MSDA	90.11 ± 07.32	76.23 ± 09.02
Gusa	(91.77 ± 05.91)	75.12 ± 07.99
ADANN	91.92 ± 05.44	73.95 ± 09.08
PR-PL	(93.06 ± 05.12)	(81.32 ± 08.53)
GDDN	92.54 ± 03.65	75.65 ± 05.47
HEDN (Ours)	93.58±06.91 (95.14±05.73)	79.82 ± 09.37 (82.81±08.95)

The best results are shown in bold, and the second best are underlined. The results shown with "()" correspond to the best session results.

1) Comparison with State-of-the-Art Methods: To validate the effectiveness of our proposed method, we compare HEDN against a comprehensive set of representative EEG emotion recognition approaches. UDDA [36] serves as a classic single-source domain adaptation baseline, while MS-MDA [10], MSDA-SFE [23], and S²A²-MSDA [18] represent standard multi-source domain adaptation methods that construct separate networks for each source-target domain pair. GUSA [37], ADANN [24] and PR-PL [22] being typical approaches that integrate prototype learning into emotion recognition. More recently, GDNN [11] has combined prototype learning with multi-source domain adaptation and further removes source domains with poor transferability to enhance robustness.

As shown in Table I, our proposed HEDN achieves the highest accuracy on both SEED, with 93.58% accuracy, and SEED-IV, with 79.82% accuracy, significantly outperforming existing methods. On the SEED dataset, HEDN surpasses the second-best method ADANN by 1.04%, while on the more challenging SEED-IV dataset, it exceeds S²A²-MSDA by 3.59%. These results demonstrate the effectiveness of our HEDN in leveraging cross-domain transferability. Notably, MSDA-SFE and GDNN achieve low standard deviations, likely due to their explicit modeling of spatial relationships between EEG channels, which improves cross-subject stability.

TABLE II
ABLATION STUDY OF HEDN ON SEED AND SEED-IV DATASETS.

Methods	SEED (%)	SEED-IV (%)	
HEDN	93.58±06.91	79.82±09.37	
Ablation study about TDA			
Random w/o Easy Source w/o Hard Source	92.20±06.92 92.34±08.14 91.60±08.09	78.71±09.10 79.19±09.96 76.28±09.72	
Ablation study about HEDN			
w/o Easy Network w/o Hard Network w/o Cluster Contrastive Loss	85.52±08.72 82.27±11.90 90.03±08.57	77.13±10.92 64.73±08.93 77.85±10.99	

TABLE III
EFFECT OF SOURCE DOMAIN NUMBER ON HEDN PERFORMANCE AND EFFICIENCY.

Sources	Accuracy (%)	Memory (KB)	Training Time (s)	Prediction Time (ms)
2	86.00	164.24	22.46	1.92
4	89.50	171.99	26.16	2.28
6	91.25	179.74	29.80	2.53
8	92.14	187.43	33.30	2.80
10	93.07	195.18	36.74	3.14
12	94.08	202.93	40.49	3.68
14	93.58	210.68	43.56	3.73

2) Ablation Study: To further investigate the contributions of individual components in our proposed method, we conduct a series of ablation experiments focusing on two key aspects: the TDA mechanism and the HEDN structure. The results are summarized in Table II.

For the TDA mechanism, we evaluate three variants: (1) Random, which selects Easy and Hard sources randomly; (2) w/o Easy Source, which uses the Hard source as both Easy and Hard; and (3) w/o Hard Source, which reuses the Easy source for both roles. Compared to the full model, the Random variant shows a moderate performance drop, indicating that principled task difficulty assessment contributes to improved generalization. Most notably, w/o Hard Source exhibits the most significant decline, as both networks are trained exclusively with Easy sources, indicating that excluding truly difficult domains reduces diversity during training and impairs convergence.

For the HEDN structure, we compare three variants: (1) w/o Hard Network, (2) w/o Easy Network, and (3) w/o Cluster Contrastive Loss. w/o Easy Network and w/o Hard Network lead to significant performance drops, highlighting their complementary roles in adaptation. The Easy Network supports knowledge transfer from easier sources, while the Hard Network plays a key role in aligning marginal distributions. Additionally, w/o Cluster Contrastive Loss moderately reduces accuracy, showing its benefit in preserving feature structures.

3) Source Number Evaluation: The number of source domains significantly affects both accuracy and efficiency in multi-source domain adaptation. We evaluate HEDN on SEED by varying the number of source domains from 2 to 14,

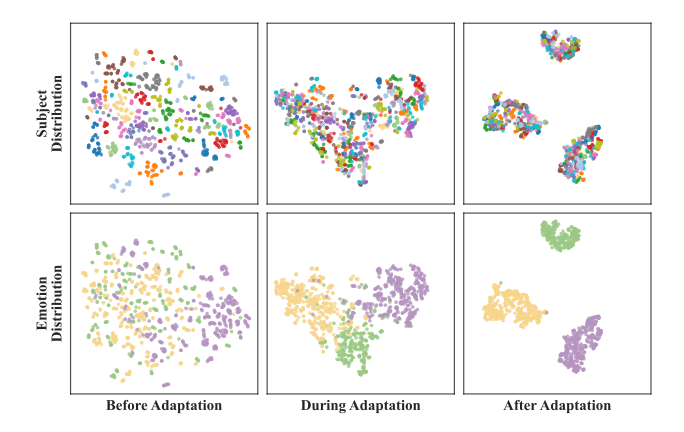


Fig. 3. t-SNE visualizations of feature distributions at different stages of adaptation.

recording average accuracy, memory consumption, training time, and prediction time, as shown in Table III.

Accuracy generally increases with the addition of more source domains, particularly when increasing from 2 to 6 domains. However, beyond 8 domains, the improvement becomes marginal, indicating diminishing returns. From a computational perspective, the benefits of reducing the number of source domains are evident. We observe a substantial decrease in training time, dropping from 43.56 seconds with 14 domains to 22.46 seconds with 2 domains. Similarly, memory usage decreases from 210.68 KB to 164.24 KB, and prediction latency significantly decreases from 3.73 milliseconds to 1.92 milliseconds. Notably, even with all 14 domains, HEDN remains lightweight and fast, proving its deployment efficiency. This makes HEDN highly suitable for real-time EEG emotion recognition on portable devices, balancing accuracy and computational cost.

4) Visualization Analysis: To intuitively demonstrate the effectiveness of our HEDN framework in aligning domain distributions and enhancing discriminative structures, we visualize feature representations at different adaptation stages using t-SNE algorithm. The top row illustrates the subject-wise distribution, where points are colored by different subjects, while the bottom row shows the emotion-wise distribution, where colors indicate different emotional categories.

As illustrated in Figure 3, the adaptation process reveals contrasting patterns between subject and emotion distributions. In the subject-wise visualization, the initial scattered distribution of different subjects gradually becomes more clustered across adaptation stages, indicating successful domain alignment where subject-specific variations are effectively minimized. Conversely, in the emotion-wise visualization, emotional categories transition from an initially mixed and overlapping state to increasingly separated and distinct clusters, demonstrating that the model progressively enhances emotion discriminability. This dual behavior—convergence of subject distributions and divergence of emotion distributions—validates that our framework successfully achieves domain alignment while preserving and enhancing task-relevant discriminative features.

V. CONCLUSION

This paper proposes a novel HEDN framework, designed to effectively address cross-subject EEG emotion recognition challenges by dynamically assessing the transfer difficulty of different source domains. Utilizing a TDA mechanism, HEDN intelligently routes source domain inputs to either a Hard Network or Easy Network, thereby achieving more precise domain adaptation. Specifically, the Hard Network handles source domains with higher transfer difficulty by aligning marginal distributions, while the Easy Network leverages prototype classification and a prototype-guided label propagation algorithm to model intra-class clustering structures and generate reliable pseudo-labels. Extensive experimental validation on SEED and SEED-IV datasets demonstrate that HEDN achieves state-ofthe-art performance, with accuracies of 93.58% and 79.82% respectively, while maintaining minimal memory usage, and prediction latency. This underscores its computational efficiency and suitability for real-time deployment on portable EEG devices. Future work will concentrate on reducing reliance on labeled target domain data and further enhancing the model's generalizability under limited supervision.

REFERENCES

- [1] C. Brunner, N. Birbaumer, B. Blankertz, C. Guger, A. Kübler, D. Mattia, J. d. R. Millán, F. Miralles, A. Nijholt, E. Opisso *et al.*, "Bnci horizon 2020: towards a roadmap for the bci community," *Brain-computer interfaces*, vol. 2, no. 1, pp. 1–10, 2015.
- [2] M. Ali, A. H. Mosa, F. Al Machot, and K. Kyamakya, "Eeg-based emotion recognition approach for e-healthcare applications," in 2016 eighth international conference on ubiquitous and future networks (ICUFN). IEEE, 2016, pp. 946–950.
- [3] X. Li, Y. Zhang, P. Tiwari, D. Song, B. Hu, M. Yang, Z. Zhao, N. Kumar, and P. Marttinen, "Eeg based emotion recognition: A tutorial and review," ACM Computing Surveys, vol. 55, no. 4, pp. 1–57, 2022.
- [4] F. Wang, W. Zhang, Z. Xu, J. Ping, and H. Chu, "A deep multi-source adaptation transfer network for cross-subject electroencephalogram emotion recognition," *Neural Computing and Applications*, vol. 33, no. 15, pp. 9061–9073, 2021.
- [5] Y. Wang, B. Zhang, and Y. Tang, "Dmmr: Cross-subject domain generalization for eeg-based emotion recognition via denoising mixed mutual reconstruction," in *Proceedings of the AAAI conference on artificial intelligence*, vol. 38, 2024, pp. 628–636.
- [6] X. Shen, X. Liu, X. Hu, D. Zhang, and S. Song, "Contrastive learning of subject-invariant eeg representations for cross-subject emotion recognition," *IEEE Transactions on Affective Computing*, vol. 14, no. 3, pp. 2496–2511, 2022.
- [7] P. Zhong, D. Wang, and C. Miao, "Eeg-based emotion recognition using regularized graph neural networks," *IEEE Transactions on Affective Computing*, vol. 13, no. 3, pp. 1290–1301, 2020.
- [8] S. Zhao, G. Wang, S. Zhang, Y. Gu, Y. Li, Z. Song, P. Xu, R. Hu, H. Chai, and K. Keutzer, "Multi-source distilling domain adaptation," in *Proceedings of the AAAI conference on artificial intelligence*, vol. 34, 2020, pp. 12 975–12 983.
- [9] J. Li, S. Qiu, Y.-Y. Shen, C.-L. Liu, and H. He, "Multisource transfer learning for cross-subject eeg emotion recognition," *IEEE transactions* on cybernetics, vol. 50, no. 7, pp. 3281–3293, 2019.
- [10] H. Chen, M. Jin, Z. Li, C. Fan, J. Li, and H. He, "Ms-mda: Multisource marginal distribution adaptation for cross-subject and cross-session eeg emotion recognition," *Frontiers in Neuroscience*, vol. 15, p. 778488, 2021
- [11] B. Chen, C. P. Chen, and T. Zhang, "Gddn: Graph domain disentanglement network for generalizable eeg emotion recognition," *IEEE Transactions on Affective Computing*, vol. 15, no. 3, pp. 1739–1753, 2024.
- [12] Y. Ma, W. Zhao, M. Meng, Q. Zhang, Q. She, and J. Zhang, "Cross-subject emotion recognition based on domain similarity of eeg signal transfer learning," *IEEE Transactions on Neural Systems and Rehabilitation Engineering*, vol. 31, pp. 936–943, 2023.

- [13] Q. Wang, L. Yang, Q. Zhang, J. Du, and Y. Ye, "Fine-grained label propagation via density-based prototype matching for cross-subject eeg emotion recognition," *Knowledge-Based Systems*, p. 114650, 2025.
- [14] L. v. d. Maaten and G. Hinton, "Visualizing data using t-sne," *Journal of machine learning research*, vol. 9, no. Nov, pp. 2579–2605, 2008.
- [15] L. Yang, Y. Balaji, S.-N. Lim, and A. Shrivastava, "Curriculum manager for source selection in multi-source domain adaptation," in *European* conference on computer vision. Springer, 2020, pp. 608–624.
- [16] Y. Mansour, M. Mohri, and A. Rostamizadeh, "Domain adaptation: Learning bounds and algorithms," arXiv preprint arXiv:0902.3430, 2009
- [17] H. Chen, Z. Li, M. Jin, and J. Li, "Meernet: Multi-source eeg-based emotion recognition network for generalization across subjects and sessions," in 2021 43rd Annual International Conference of the IEEE Engineering in Medicine & Biology Society (EMBC). IEEE, 2021, pp. 6094–6097.
- [18] Y. Yang, Z. Wang, W. Tao, X. Liu, Z. Jia, B. Wang, and F. Wan, "Spectral-spatial attention alignment for multi-source domain adaptation in eeg-based emotion recognition," *IEEE Transactions on Affective Computing*, vol. 15, no. 4, pp. 2012–2024, 2024.
- [19] Q. She, Y. Cai, S. Du, and Y. Chen, "Multi-source manifold feature transfer learning with domain selection for brain-computer interfaces," *Neurocomputing*, vol. 514, pp. 313–327, 2022.
- [20] J. Wang, X. Ning, W. Xu, Y. Li, Z. Jia, and Y. Lin, "Multi-source selective graph domain adaptation network for cross-subject eeg emotion recognition," *Neural Networks*, vol. 180, p. 106742, 2024.
- [21] H.-M. Yang, X.-Y. Zhang, F. Yin, and C.-L. Liu, "Robust classification with convolutional prototype learning," in *Proceedings of the IEEE* conference on computer vision and pattern recognition, 2018, pp. 3474– 3482.
- [22] R. Zhou, Z. Zhang, H. Fu, L. Zhang, L. Li, G. Huang, F. Li, X. Yang, Y. Dong, Y.-T. Zhang et al., "Pr-pl: A novel prototypical representation based pairwise learning framework for emotion recognition using eeg signals," *IEEE Transactions on Affective Computing*, vol. 15, no. 2, pp. 657–670, 2023.
- [23] W. Guo, G. Xu, and Y. Wang, "Multi-source domain adaptation with spatio-temporal feature extractor for eeg emotion recognition," *Biomedical Signal Processing and Control*, vol. 84, p. 104998, 2023.
- [24] X. Hong, C. Du, and H. He, "Adaptive domain alignment neural networks for cross-domain eeg emotion recognition," *IEEE Transactions* on Affective Computing, 2024.
- [25] J. Blitzer, K. Crammer, A. Kulesza, F. Pereira, and J. Wortman, "Learning bounds for domain adaptation," *Advances in neural information processing systems*, vol. 20, 2007.
- [26] Y. Ganin, E. Ustinova, H. Ajakan, P. Germain, H. Larochelle, F. Laviolette, M. March, and V. Lempitsky, "Domain-adversarial training of neural networks," *Journal of machine learning research*, vol. 17, no. 59, pp. 1–35, 2016.
- [27] S. Liu, Z. Wang, Y. An, B. Li, X. Wang, and Y. Zhang, "Da-capsnet: A multi-branch capsule network based on adversarial domain adaption for cross-subject eeg emotion recognition," *Knowledge-Based Systems*, vol. 283, p. 111137, 2024.
- [28] D. Abdolzadegan, M. H. Moattar, and M. Ghoshuni, "A robust method for early diagnosis of autism spectrum disorder from eeg signals based on feature selection and dbscan method," *Biocybernetics and Biomedical Engineering*, vol. 40, no. 1, pp. 482–493, 2020.
- [29] S. Xie, Z. Zheng, L. Chen, and C. Chen, "Learning semantic representations for unsupervised domain adaptation," in *International conference* on machine learning. PMLR, 2018, pp. 5423–5432.
- [30] K. He, H. Fan, Y. Wu, S. Xie, and R. Girshick, "Momentum contrast for unsupervised visual representation learning," in *Proceedings of the IEEE/CVF conference on computer vision and pattern recognition*, 2020, pp. 9729–9738.
- [31] P. Khosla, P. Teterwak, C. Wang, A. Sarna, Y. Tian, P. Isola, A. Maschinot, C. Liu, and D. Krishnan, "Supervised contrastive learning," Advances in neural information processing systems, vol. 33, pp. 18 661–18 673, 2020.
- [32] R. Wood, E. Domingo, V. H. Koelzer, T. S. Maughan, and J. Rittscher, "Cluster triplet loss for unsupervised domain adaptation on histology images," in *Proceedings of the IEEE/CVF Conference on Computer Vision and Pattern Recognition*, 2024, pp. 5122–5131.
- [33] W.-L. Zheng and B.-L. Lu, "Investigating critical frequency bands and channels for eeg-based emotion recognition with deep neural networks," *IEEE Transactions on autonomous mental development*, vol. 7, no. 3, pp. 162–175, 2015.

- [34] W.-L. Zheng, W. Liu, Y. Lu, B.-L. Lu, and A. Cichocki, "Emotionmeter: A multimodal framework for recognizing human emotions," *IEEE transactions on cybernetics*, vol. 49, no. 3, pp. 1110–1122, 2018.
- [35] R.-N. Duan, J.-Y. Zhu, and B.-L. Lu, "Differential entropy feature for eeg-based emotion classification," in 2013 6th international IEEE/EMBS conference on neural engineering (NER). IEEE, 2013, pp. 81–84.
- [36] Z. Li, E. Zhu, M. Jin, C. Fan, H. He, T. Cai, and J. Li, "Dynamic domain adaptation for class-aware cross-subject and cross-session eeg emotion recognition," *IEEE Journal of Biomedical and Health Informatics*, vol. 26, no. 12, pp. 5964–5973, 2022.
- [37] X. Li, C. P. Chen, B. Chen, and T. Zhang, "Gusa: Graph-based unsuper-vised subdomain adaptation for cross-subject eeg emotion recognition," IEEE Transactions on Affective Computing, vol. 15, no. 3, pp. 1451–1462, 2024.